^{64}Cu-DOTATATE PET in Patients with Neuroendocrine Neoplasms: Prospective, Head-to-Head Comparison of Imaging at 1 Hour and 3 Hours After Injection

Mathias Loft[1,2], Esben A. Carlsen[1,2], Camilla B. Johnbeck[1,2], Helle H. Johannesen[1,2], Tina Binderup[1,2], Andreas Pfeifer[1,2], Jann Mortensen[1,2], Peter Oturai[1,2], Annika Loft[1,2], Anne K. Berthelsen[1,2], Seppo W. Langer[2,3], Ulrich Knigge[2,4], and Andreas Kjaer[1,2]

[1]Department of Clinical Physiology, Nuclear Medicine, and PET and Cluster for Molecular Imaging, Department of Biomedical Sciences, Rigshospitalet and University of Copenhagen, Copenhagen, Denmark; [2]ENETS Neuroendocrine Tumor Center of Excellence, Rigshospitalet, Copenhagen, Denmark; [3]Department of Oncology, Rigshospitalet, Copenhagen, Denmark; and [4]Departments of Clinical Endocrinology and Surgical Gastroenterology, Rigshospitalet, Copenhagen, Denmark

^{64}Cu-DOTATATE PET/CT imaging 1 h after injection is excellent for lesion detection in patients with neuroendocrine neoplasms (NENs). We hypothesized that the imaging time window can be extended up to 3 h after injection without significant differences in the number of lesions detected. **Methods:** From a prospective study, we compared, on a head-to-head basis, sets of ^{64}Cu-DOTATATE PET/CT images from 35 patients with NENs scanned 1 and 3 h after injection of 200 MBq of ^{64}Cu-DOTATATE. The number of lesions on both PET scans was counted and grouped according to organs or regions and compared with negative binomial regression. Discordant lesions (visible on only the 1-h images or only the 3-h ^{64}Cu-DOTATATE PET images) were considered true if found on simultaneous CT or later MR, CT, or somatostatin receptor imaging. We measured lesion SUV_{max}, reference normal-organ or -tissue SUV_{mean}, and tumor–to–normal-tissue ratios calculated from SUV_{max} and SUV_{mean}. **Results:** We found 822 concordant lesions (visible on both 1-h and 3-h ^{64}Cu-DOTATATE PET) and 5 discordant lesions, of which 4 were considered true. One discordant case in 1 patient involved a discordant organ system (lymph node) detected on 3-h but not 1-h ^{64}Cu-DOTATATE PET that did not alter the patient's disease stage (stage IV) because the patient had 11 additional concordant liver lesions. We found no significant differences between the number of lesions detected on 1-h and 3-h ^{64}Cu-DOTATATE PET. Throughout the 1- to 3-h imaging window, the mean tumor–to–normal-tissue ratio remained high in all key organs: liver (1 h: 12.6 [95% confidence interval (CI), 10.2–14.9]; 3 h: 11.0 [95%CI, 8.7–13.4]), intestines (1 h: 24.2 [95%CI, 14.9–33.4]; 3 h: 28.2 [95%CI, 16.5–40.0]), pancreas (1 h: 42.4 [95%CI, 12.3–72.5]; 3 h: 41.1 [95%CI, 8.7–73.4]), and bone (1 h: 103.0 [95%CI, 38.6–167.4]; 3 h: 124.2 [95% CI, 57.1–191.2]). **Conclusion:** The imaging time window of ^{64}Cu-DOTATATE PET/CT for patients with NENs can be expanded from 1 h to 1–3 h without significant differences in the number of lesions detected.

Key Words: ^{64}Cu-DOTATATE; somatostatin receptor imaging; SUV; PET/CT; neuroendocrine neoplasms

J Nucl Med 2021; 62:73–80
DOI: 10.2967/jnumed.120.244509

Neuroendocrine neoplasms (NENs) represent a heterogeneous class of diseases with large variability in aggressiveness and prognosis. NENs most frequently originate from the pancreas, the gastrointestinal tract, or the lung (*1*). A common feature of most NENs is the overexpression of somatostatin receptors (SSTRs) (*2,3*), and SSTR imaging with radioactively labeled SSTR-specific peptides plays an important role in the staging, follow-up, and treatment guidance of patients with NENs (*4–7*).

We have previously demonstrated that SSTR-targeting PET imaging 1 h after injection of 200 MBq of ^{64}Cu-DOTATATE is excellent in lesion detection in patients with NENs, compared with other clinically available ^{68}Ga-based PET and ^{111}In-based SPECT SSTR-imaging modalities (*8,9*). Accordingly, in 2018 ^{64}Cu-DOTATATE PET was introduced at Rigshospitalet, Copenhagen, Denmark, as routine SSTR imaging for patients with NENs.

^{64}Cu has a low maximal positron energy (0.653 MeV) resulting in a short mean positron range (0.6 mm) that leads to excellent image resolution (*10*). For comparison, the mean positron range of ^{68}Ga is 2.9 mm (*11*). In addition, ^{64}Cu has the advantage of a longer half-life than ^{68}Ga (12.7 h vs. 68 min), which prolongs the postsynthesis use time of ^{64}Cu-based tracers compared with ^{68}Ga-based tracers. This advantage allows for central production of the tracer at a ^{64}Cu-cyclotron site, and the tracer can then be distributed to other nonproduction sites with sufficient activity left at time of injection. The shelf life of ^{64}Cu-DOTATATE is 24 h (*12*), making it possible to prepare the tracer on one day and inject and image patients on the following day.

The long ^{64}Cu half-life also makes it possible to perform imaging in a broader time window and up to several hours after injection with sufficient count statistics on later scans. An obvious benefit of the flexibility in acquisition timing is the possibility to complete a scan of an already injected patient if delays occur such that the scan cannot be completed at the target time (1 h after injection). Initial analysis from our first-in-humans study with ^{64}Cu-DOTATATE suggested that the imaging window could be extended up to at least 3 h after injection without loss of image quality or tumor detection ability (*12*). However, the study included a relatively small number of patients, and no formal quantitative analysis on the lesion numbers was performed.

Received Mar. 6, 2020; revision accepted Apr. 24, 2020.
For correspondence or reprints contact: Andreas Kjaer, Department of Clinical Physiology, Nuclear Medicine, and PET, KF-4011, Rigshospitalet, Blegdamsvej 9, DK-2100 Copenhagen, Denmark.
E-mail: akjaer@sund.ku.dk
Published online May 22, 2020.

The aim of the current study was therefore to compare quantitatively, on a head-to-head basis, ^{64}Cu-DOTATATE PET/CT scans for tumor lesion detection in patients with NENs scanned at 1 and 3 h after injection in a larger group of patients. We hypothesized that the imaging time window can be expanded from 1 h to 3 h without significant differences in the number of lesions detected.

MATERIALS AND METHODS

Patients and Study Design

The study was part of our previously published prospective study of patients with NENs scanned with ^{64}Cu-DOTATATE PET/CT at Rigshospitalet, Copenhagen, Denmark, from 2009 to 2013 (*8*). In that study, the first 35 patients were scanned using ^{64}Cu-DOTATATE PET/CT both at 1 h and at 3 h after injection, and these 35 sets of scans were included in the current head-to-head analysis. Patients were characterized by sex, age, primary tumor location, tumor functional status, tumor grade, and previous NEN-related treatments. All patients had provided written informed consent before inclusion. The study was approved by the Regional Scientific Ethical Committee (reference no. H-D-2008-045).

TABLE 1
Patient Characteristics

Characteristic	Data
Sex	
Male	21 (60%)
Female	14 (40%)
Age (y)	
Mean	62
Range	40–81
Site of primary tumor	
Lung	3 (9%)
Gastrointestinal	13 (37%)
Pancreatic	5 (14%)
Other	2 (6%)
Unknown	12 (34%)
Functional status	
Nonfunctioning	20 (57%)
Functioning (carcinoid syndrome)	15 (43%)
Grade	
Low (G1)	8 (23%)
Intermediate (G2)	21 (60%)
High (G3)	2 (6%)
KI-67 proliferation index not available	4 (11%)
Primary tumor removed	
No	20 (57%)
Yes	15 (43%)
Previous treatments*	
Surgery	15 (43%)
Interferon α	19 (54%)
Somatostatin analogs	14 (40%)
Radiofrequency ablation (liver metastases)	3 (9%)
External radiation therapy	1 (3%)
Peptide receptor radionuclide therapy	12 (34%)

*Some patients received multiple treatments. Therefore, total number of treatments exceeded number of patients.

Data are *n* followed by percentage in parentheses, except for age.

TABLE 2
Lesions per Organ or Region

Organ or tissue	Visible on ^{64}Cu-DOTATATE PET: Concordant	Only at 1 h after injection	Only at 3 h after injection	$P^{\dagger}$
Lung	14	0	0	—
Liver	298	0	2	0.98
Intestines	18	0	0	—
Pancreas	12	0	0	—
Intraabdominal carcinomatosis	7	0	0	—
Bone	326	1	1	1.00
Lymph nodes	114	0	1	0.98
Other*	33	0	0	—
Total	822	1	4	0.99

*22 soft-tissue lesions, 5 heart lesions, 1 prostate lesion, 1 adrenal lesion, 1 stomach lesion, 1 thyroid lesion, 1 brain lesion, and 1 spleen lesion.

†Testing for differences in number of lesions with negative binominal regression on ^{64}Cu-DOTATATE PET between 1 and 3 h after injection. The analyses are performed per organ or region and on the total number of lesions.

Radiotracer Synthesis and Image Acquisition

The ^{64}Cu-DOTATATE production and PET/CT imaging have previously been described in detail (*8,12*). In brief, ^{64}Cu-DOTATATE was produced in-house, and the injected activity was approximately 200 MBq. Subsequent whole-body PET imaging (from skull to mid-thigh) was performed at 1 and 3 h after injection. The axial and transaxial fields of view were 216 and 205 mm, respectively, and the acquisition time was 3 min per bed position. All patients were scanned on a Biograph 64 TruePoint PET/CT scanner (Siemens Medical Solutions), and the PET data were reconstructed with the TrueX algorithm (Siemens Medical Solutions) using 3 iterations and 21 subsets and smoothed by a gaussian filter (2 mm in full width at half maximum). Before the 1-h PET scan, a diagnostic CT scan was acquired with the following settings: 3-mm slice thickness, 120 kV, and a quality reference of 225 mA modulated by the Care Dose 4D automatic exposure control system (Siemens Medical Solutions). Unless contraindicated, patients received 75 mL of iodine-containing contrast agent administered by an automatic infusion system (Optiray 300; Covidien) with scan delays of 60 s (flow rate, 1.5 mL/s) followed by an infusion of 100 mL of NaCl (flow rate, 2.5 mL/s). The diagnostic CT scan was used for attenuation correction of the 1-h PET scan. Before the subsequent 3-h PET scan, a low-dose CT scan (20 mA, 140 kV) without a contrast agent was acquired for attenuation correction.

TABLE 3
Discordant Lesions per Patient

Patient no.	Visible on ^{64}Cu-DOTATATE PET			Status	Months until follow-up	Follow-up image modality	Discordant organ system
	Concordant	Only at 1 h after injection	Only at 3 h after injection				
1	Liver (11)		LN (1)	TP	0*/9	CT/Cu	LN
2	Bone (15), LN (7), lung (1), carc (1), liver (43)	Bone (1)		FP	8	CT	None
3	Liver (6), LN (8), int (1)		Liver (1)	TP	46/46	Ga/CT	None
4	Bone (19), spleen (1), int (1), adrenal (1), heart (3), liver (5)		Bone (1)	TP	0*	CT	None
5	Liver (2), LN (19) heart (2), int (1)		Liver (1)	TP	39	Ga	None

*Visible CT correlate on ^{64}Cu-DOTATATE PET/CT.

LN = lymph nodes; TP = true-positive; Cu = follow-up ^{64}Cu-DOTATATE PET at 1 h after injection; carc = intraabdominal carcinomatosis; FP = false-positive; int = intestines; Ga = ^{68}Ga-DOTATOC PET.

Imaging Analysis

The 1- and 3-h ^{64}Cu-DOTATATE PET/CT scans were reviewed side by side from June to August 2019 by the same SSTR reader in cooperation with a radiologist masked to the previous imaging analysis. All foci were identified on PET, and the CT scan was used mainly to confirm the anatomic location of the PET foci. Lesion sites were divided into organs or regions: liver, pancreas, intestines, lung/pleura, bones, lymph nodes, intraabdominal carcinomatosis, and other (soft tissue, heart, stomach, adrenal, and other less common regions), and all PET-positive lesions (defined as a clearly detectable lesion distinguishable from the surrounding tissue or organ) in each organ or region were counted. The concordance of the lesions on 1- and 3-h ^{64}Cu-DOTATATE PET was assessed for each organ or region. Discordant findings were followed up until October 2019 (≤10 y of follow-up) using available MR, CT, or SSTR images to determine whether the discordant finding was a true lesion. A discordant finding was considered true if the lesion had a visible CT correlate on 1- or 3-h ^{64}Cu-DOTATATE PET/CT or could be found on a later SSTR-imaging modality or other imaging methods on follow-up.

To establish a set of reference uptake values for the ^{64}Cu-DOTATATE PET images in patients with NENs, we also quantified uptake in lesions and normal organs and tissues on both the 1-h and the 3-h ^{64}Cu-DOTATATE PET images. The SUV_{max} of the hottest

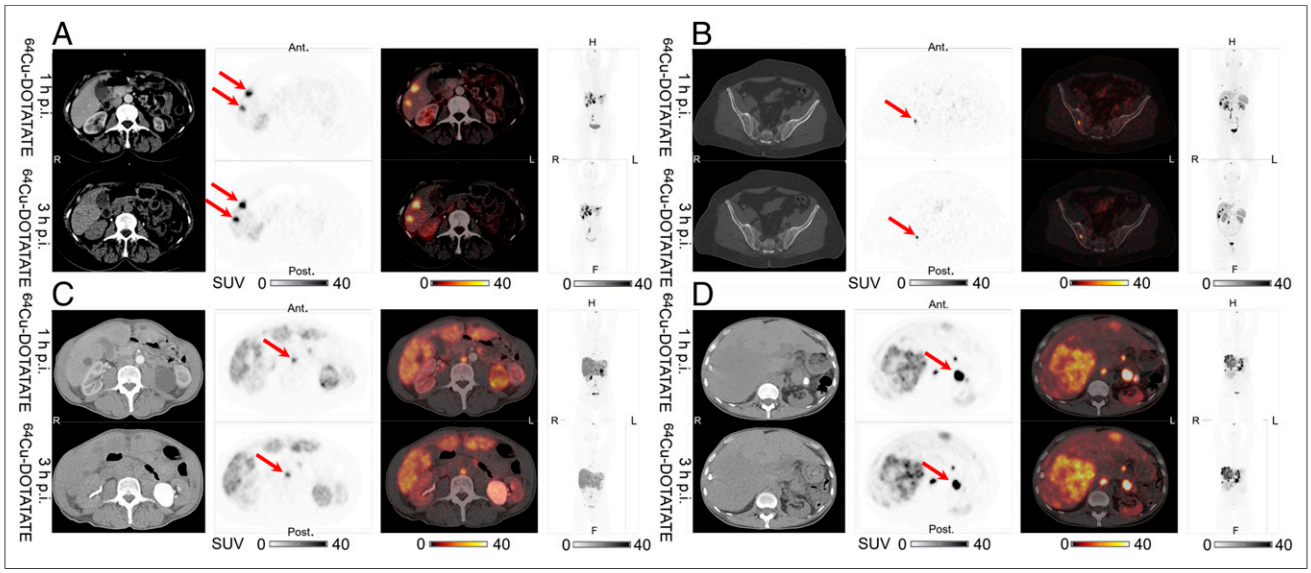

FIGURE 1. Representative examples of liver lesions (A), bone lesions (B), lymph node lesions (C), and pancreatic lesions (D) in same patients scanned at 1 and 3 h after injection. From left to right are shown CT, ^{64}Cu-DOTATATE PET, ^{64}Cu-DOTATATE PET/CT, and maximum-intensity projection, with corresponding SUV color bars below. All lesions were identified at both 1 h and 3 h on ^{64}Cu-DOTATATE PET (arrows). Ant = anterior; F = feet; H = head; p.i. = after injection; post = posterior.

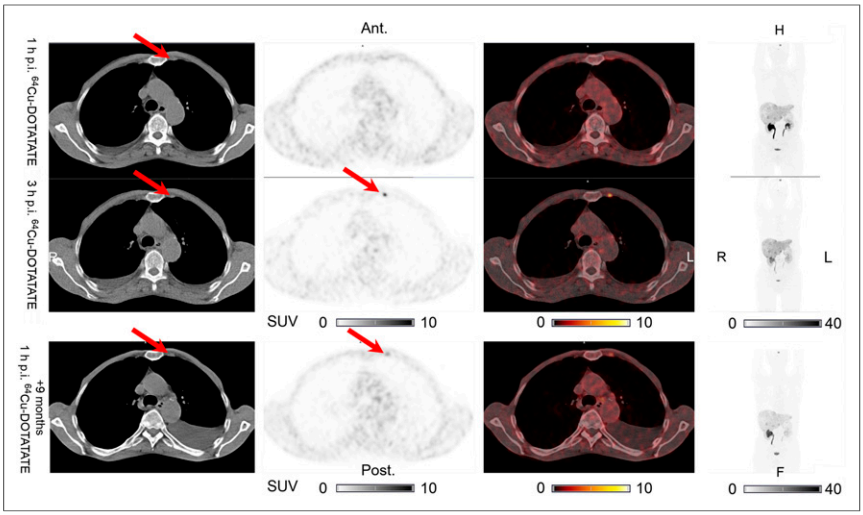

FIGURE 2. True-positive finding in patient 1: one additional lymph node lesion (arrows) visible on ^{64}Cu-DOTATATE PET at 3 h after injection but not at 1 h, with visible CT correlate. Lesion was also visible on PET and CT at 1 h after injection on ^{64}Cu-DOTATATE PET/CT performed 9 mo later. From left to right are shown CT, ^{64}Cu-DOTATATE PET, ^{64}Cu-DOTATATE PET/CT, and maximum-intensity projection, with corresponding SUV color bars below. Ant = anterior; F = feet; H = head; p.i. = after injection; post = posterior.

concordant lesion, if any, in each organ or region was measured from a region of interest covering the entire lesion. The SUV_{mean} of the reference organs or tissues was measured from spheric regions of interest on a nondiseased area of the right liver lobe, the lung adjacent to the right hilus, the cauda and uncinate process of the pancreas, the spleen, the intestines (ileum), the gluteal muscle, and an area 5 cm below the trochanter of the right femur for a bone reference. Reference values for the pituitary gland and the adrenal glands were measured with the SyngoVIA (version VB30A-HF04; Siemens Medical Solutions) isocontour region-of-interest tool (default threshold, 40% of maximum) for a region of interest covering the entire organ. Tumor–to–normal-tissue ratios (TTN) for lesions in the liver, pancreas, and lung were calculated by dividing the lesion SUV_{max} by the SUV_{mean} of the nondiseased area in the corresponding organ. Similarly, the femur SUV_{mean} was used for bone TTN, intestinal SUV_{mean} for intestinal and intraabdominal carcinomatosis TTN, and gluteal muscle SUV_{mean} for lymph node TTN. All images were analyzed using SyngoVIA.

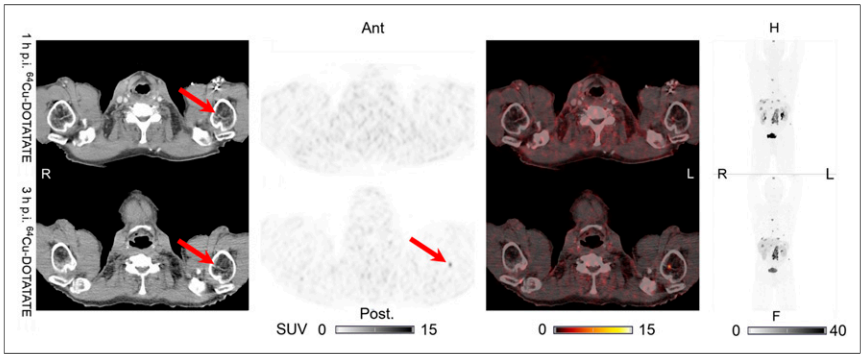

FIGURE 3. True-positive finding in patient 4: one additional bone lesion (arrows) visible on ^{64}Cu-DOTATATE PET at 3 h after injection but not at 1 h, with visible CT correlate. No later SSTR PET images were available. From left to right are shown CT, ^{64}Cu-DOTATATE PET, ^{64}Cu-DOTATATE PET/CT, and maximum-intensity projection, with corresponding SUV color bars below. Ant = anterior; F = feet; H = head; p.i. = after injection; post = posterior.

Statistical Methods

Differences in the number of lesions between 1- and 3-h ^{64}Cu-DOTATATE PET were analyzed with negative binomial regression. The 1- and 3-h ^{64}Cu-DOTATATE PET lesion SUV_{max}, reference organ and tissue SUV_{mean}, and TTN are shown as mean with 95% confidence intervals and were analyzed with paired *t* tests adjusted for multiple comparisons by Bonferroni adjustments (*13*). Two-sided *P* values of less than 0.05 were considered statistically significant. All statistical analyses were performed using R statistical software (version 3.6.1; R Foundation for Statistical Computing).

RESULTS

Patient and Imaging Characteristics

The mean injected dose of ^{64}Cu-DOTATATE was 205 MBq (range, 183–232 MBq). Tracer uptake time was 52.9 min (range, 43–80 min) and 180.0 min (range, 167–194 min) for 1- and 3-h ^{64}Cu-DOTATATE PET, respectively. The characteristics of the patients are shown in Table 1.

Lesion Numbers

The 1- and 3-h ^{64}Cu-DOTATATE PET images were of excellent quality, with detection of most lesions on both scans. Figure 1 shows representative examples of patients with detectable lesions on both 1-h and 3-h ^{64}Cu-DOTATATE PET in different organs: liver (Fig. 1A), bone (Fig. 1B), lymph nodes (Fig. 1C), and pancreas (Fig. 1D). Lesions divided into organs and regions are shown in Table 2. In total, 822 lesions (99.4% of all lesions) were identified on both 1-h and 3-h ^{64}Cu-DOTATATE PET (concordant lesions), whereas 5 lesions (0.6% of all lesions) were identified on one of the PET scans but not the other (discordant lesions). No significant differences in the number of lesions per organ or region or in the total number of lesions were found. Table 3 shows discordant findings on a per-patient basis. The 5 discordant lesions were detected in 5 different patients. In 4 of these cases, the discordant lesion was present on 3-h but not 1-h ^{64}Cu-DOTATATE PET. Two of the discordant lesions (lymph node in patient 1 and bone in patient 4) had visible CT correlates on ^{64}Cu-DOTATATE PET/CT and were thus considered true-positive (Figs. 2 and 3). Two additional discordant findings (liver in patients 3 and 5) were considered true-positive since they could be identified on later ^{68}Ga-DOTATOC PET (Figs. 4 and 5). The remaining discordant lesion (bone in patient 2) was considered false-positive since the lesion could not be identified on later imaging modalities (Fig. 6). One of the discordant lesions (lymph node in patient 1) revealed, on the 3-h ^{64}Cu-DOTATATE PET, involvement of an additional organ system not detected on the 1-h PET. This patient had 11 additional concordant metastatic liver lesions.

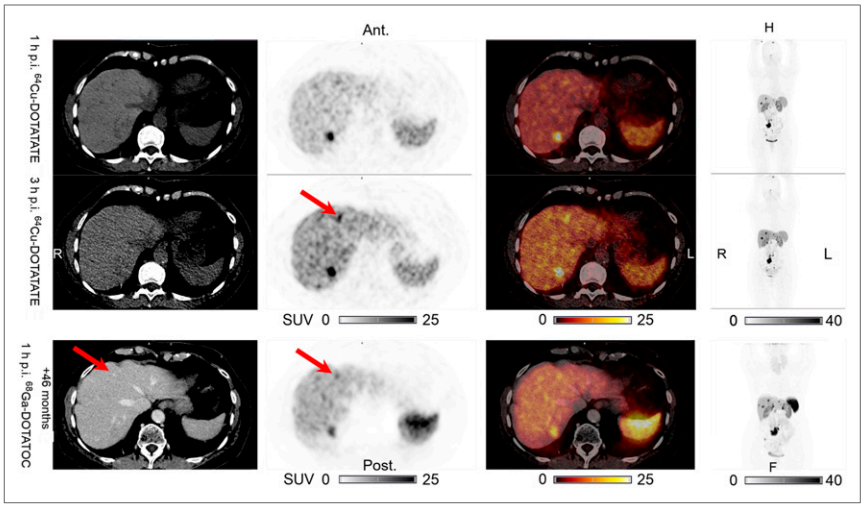

FIGURE 4. True-positive finding in patient 3: one additional liver lesion (arrows) visible on ^{64}Cu-DOTATATE PET at 3 h after injection but not at 1 h, without CT correlate. This discordant lesion was also visible on PET and CT at 1 h after injection on ^{68}Ga-DOTATOC PET performed 46 mo later. From left to right are shown CT, ^{64}Cu-DOTATATE PET (^{68}Ga-DOTATOC PET), ^{64}Cu-DOTATATE PET/CT (^{68}Ga-DOTATOC PET/CT), and maximum-intensity projection, with corresponding SUV color bars below. Ant = anterior; F = feet; H = head; p.i. = after injection; post = posterior.

Quantitative Image Analysis

Lesion SUV_{max} divided into organs and regions is shown in Table 4, and the SUV_{mean} of normal organs and tissues is shown in Table 5. Table 6 shows the lesion TTN in patients with both lesions and evaluable normal tissue in the corresponding organ or region.

DISCUSSION

In this prospective study, we investigated the hypothesis that ^{64}Cu-DOTATATE PET may be performed from 1 to 3 h after injection without loss of the lesion detection ability that is possible with 1-h imaging. Our main finding was that ^{64}Cu-DOTATATE can be used for PET imaging of patients with NENs from 1 to 3 h after injection, with high TTN (lesion contrast) and a stable lesion detection rate and no significant differences in the number of lesions detected. In comparison with the fixed image acquisition 1 h after injection of ^{68}Ga-labeled SSTR PET tracers the expansion of the acquisition time window of ^{64}Cu-DOTATATE PET is convenient in daily clinical routine.

The high agreement in the number of lesions and organ systems detected on both 1-h and 3-h ^{64}Cu-DOTATATE PET supports the rationale for expanding the imaging time window. The 2 additional true-positive liver lesions found on 3-h ^{64}Cu-DOTATATE PET further suggests that in difficult cases with clinical suspicion of a small liver focus, it might be advantageous to perform late-phase ^{64}Cu-DOTATATE PET at 3 h after injection if nothing is found on 1-h ^{64}Cu-DOTATATE PET. Of the 5 discordant lesions, only 1 revealed—on the 3-h ^{64}Cu-DOTATATE PET—involvement of an additional organ system (lymph node in patient 1) not seen on the 1-h PET. Since the patient had 11 concordant metastatic liver lesions, the patient's disease stage would not have changed from stage IV as a consequence of the additional lymph node detected on 3-h ^{64}Cu-DOTATATE PET (*14*). However, the finding of an additional extrahepatic lesion in a patient with liver-only lesions could potentially have an impact on clinical management. In the remaining 4 cases, the discordant findings involved lesions in already-concordant organ systems.

The relatively short follow-up between the ^{64}Cu-DOTATATE PET/CT and the latest available CT for patient 2 (8 mo) may explain why the discordant bone lesion could not be confirmed. For ^{64}Cu-DOTATATE (*8,9*), ^{68}Ga-DOTATOC (*15*), and ^{68}Ga-DOTATATE (*16*), bone lesions are detected on PET several months to years before detection on CT in some cases. Alternatively, the finding may represent an artifact on 1-h ^{64}Cu-DOTATATE PET. Importantly, the patient also had several concordant bone lesions. The clinical consequences of the false-positive findings are very limited.

It has been questioned whether the ^{64}Cu-DOTATATE liver uptake could present a challenge for detection of liver lesions. Although a numeric increase in the mean liver SUV_{mean} on the 3-h, compared with the 1-h, ^{64}Cu-DOTATATE PET was seen, the median liver SUV_{mean} for ^{64}Cu-DOTATATE in our study (3.86 at 1 h and 5.52 at 3 h after injection) was still lower at both time points than what has been reported for

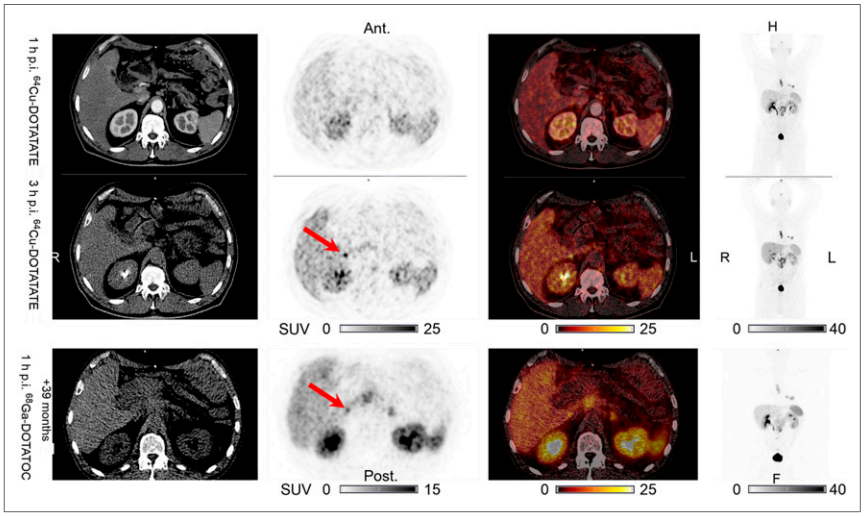

FIGURE 5. True-positive finding in patient 5: one additional liver lesion (arrows) visible on ^{64}Cu-DOTATATE PET at 3 h after injection but not at 1 h, with no visible CT correlate. This discordant lesion was also visible on PET without CT correlate at 1 h after injection on ^{68}Ga-DOTATOC PET/CT performed 39 mo later. From left to right are shown CT, ^{64}Cu-DOTATATE PET (^{68}Ga-DOTATOC PET), ^{64}Cu-DOTATATE PET/CT(^{68}Ga-DOTATOC PET/CT), and maximum-intensity projection, with corresponding SUV color bars below. Ant = anterior; F = feet; H = head; p.i. = after injection; post = posterior.

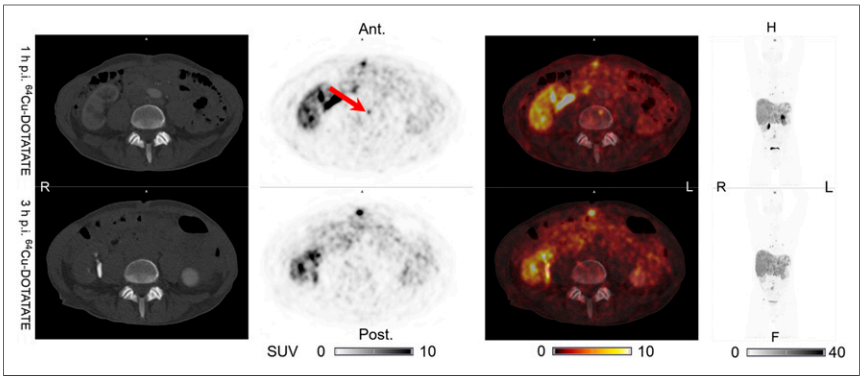

FIGURE 6. False-positive finding in patient 2: one additional bone lesion (arrow) visible on ^{64}Cu-DOTATATE PET at 1 h after injection but not at 3 h, without CT correlate. No later SSTR PET images were available. No visible CT correlate was seen on latest CT scan, 8 mo later (not shown). From left to right are shown CT, ^{64}Cu-DOTATATE PET, ^{64}Cu-DOTATATE PET/CT, and maximum-intensity projection, with corresponding SUV color bars below. Ant = anterior; F = feet; H = head; p.i. = after injection; post = posterior.

another ^{64}Cu-labeled SSTR PET tracer, ^{64}Cu-MeCOSar-Tyr^3-octreotate (7.10 at 1 h and 5.90 at 4 h after injection) (*17*). The mean liver SUV_{mean} at both 1 h and 3 h for ^{64}Cu-DOTATATE was also within the range of, or lower than, that reported for ^{68}Ga-DOTATATE at 1 h after injection: 4.5 (*18*) to 7.2 (*19*). In addition, because the liver lesion SUV_{max} also increased from the 1-h to the 3-h ^{64}Cu-DOTATATE PET, the mean liver TTN remained high and almost unchanged from 1 to 3 h after injection (12.6 vs. 11.0). Moreover, and importantly, the liver lesion detection ability at 3 h after injection was not affected, as 2 additional true liver lesions were identified on 3-h ^{64}Cu-DOTATATE PET. Although it is open to discussion whether the use of 2 different CT scans for attenuation correction for the 1- and 3-h ^{64}Cu-DOTATATE PET could have contributed to differences in quantification at the 2 time points, we find this possibility unlikely to have had any clinical relevance (*20,21*).

It might be speculated whether differences in liver background and liver lesion uptake between the 1- and 3-h ^{64}Cu-DOTATATE PET should be considered when ^{64}Cu-DOTATATE PET is used to select patients for peptide receptor radionuclide therapy (PRRT). However, apart from a single bone lesion, all lesions in all patients were above liver background uptake both at 1 h and at 3 h after injection. Therefore, if a modified Krenning scale had been applied, the conclusions would be similar whether based on 1-h or 3-h ^{64}Cu-DOTATATE PET. However, if more quantitative cutoffs are established for guiding PRRT, they are likely to be both PET tracer–specific and scan time–specific.

The high TTNs measured on both 1-h and 3-h ^{64}Cu-DOTATATE PET throughout the different organs and regions suggest that tumor delineation from the surroundings remains sufficient in the 1- to 3-h time window. Combined with the high concordance in the number of lesions detected on both 1-h and 3-h ^{64}Cu-DOTATATE PET, this observation supports the conclusion that no clinically relevant loss in image information occurs within the 1- to 3-h imaging window.

TABLE 4
Lesion SUV_{max}

Organ or tissue	*n**	Lesion SUV_{max} on ^{64}Cu-DOTATATE PET: 1 h after injection	3 h after injection	*P*†
Lung	5	17.9 [3.0–32.9]	18.7 [5.3–32.1]	1.00
Liver	22	45.7 [37.2–54.3]	54.1 [44.3–64.0]	<0.01
Intestines	12	64.4 [43.9–84.8]	77.8 [52.3–103.3]	0.19
Pancreas	8	79.0 [38.3–119.6]	85.9 [35.9–135.8]	1.00
Bone	12	44.2 [25.7–62.7]	50.1 [29.7–70.4]	0.46
Intraabdominal carcinomatosis	4	23.0 [7.7–38.3]	24.9 [9.0–40.7]	1.00
Lymph nodes	18‡	40.9 [26.9–54.9]	43.5 [29.1–58.0]	0.76

*Number of patients with lesions.
†Paired *t* testing with Bonferroni adjustment for multiple comparisons (n = 7) and capped at 1.00.
‡n = 19 on ^{64}Cu-DOTATATE PET at 3 h after injection (one additional lymph node lesion detected in 1 patient).
Data are mean values followed by 95% confidence interval in brackets.

TABLE 5
Normal-Organ SUV_{mean}

Organ or tissue	*n**	Normal-organ SUV_{mean}† on ^{64}Cu-DOTATATE PET: 1 h after injection	3 h after injection	*P*†
Lung	35	0.27 [0.23–0.30]	0.15 [0.13–0.17]	<0.01
Liver	32	4.0 [3.6–4.4]	5.7 [5.2–6.3]	<0.01
Intestines	35	2.6 [2.1–3.1]	2.5 [2.0–3.1]	1.00
Uncinate process of pancreas	31	3.2 [2.7–3.6]	3.3 [2.7–3.9]	1.00
Cauda of pancreas	32	3.1 [2.8–3.5]	3.5 [3.2–3.9]	0.38
Bone	35	0.76 [0.66–0.85]	0.64 [0.56–0.73]	<0.01
Muscle	35	0.63 [0.57–0.69]	0.49 [0.44–0.54]	<0.01
Spleen	35	8.9 [7.8–10.0]	9.3 [8.2–10.4]	0.12
Pituitary gland	35	12.9 [10.8–14.9]	15.8 [13.4–18.2]	<0.01
Adrenal gland	33	9.5 [8.0–11.0]	9.9 [8.2–11.6]	1.00

*Number of patients with evaluable normal organs.
†Paired *t* testing with Bonferroni adjustment for multiple comparisons (n = 10) and capped at 1.00.
Data are mean values followed by 95% confidence interval in brackets.

TABLE 6
TTN

Organ or tissue	n*	TTN†		P†
		1 h after injection of ^{64}Cu-DOTATATE	3 h after injection of ^{64}Cu-DOTATATE	
Lung	5	87.9 [30.2–145.6]	160.9 [79.2–242.6]	0.04
Liver	19	12.6 [10.2–14.9]	11.0 [8.7–13.4]	0.03
Intestines	12	24.2 [14.9–33.4]	28.2 [16.5–40.0]	0.73
Pancreas	6	42.4 [12.3–72.5]	41.1 [8.7–73.4]	1.00
Bone	12	103.0 [38.6–167.4]	124.2 [57.1–191.2]	0.07
Intraabdominal carcinomatosis	4	14.0 [3.0–25.0]	22.5 [7.1–38.0]	0.50
Lymph nodes	18‡	73.7 [43.0–104.4]	94.0 [61.6–126.4]	0.07

*Number of patients with lesions and evaluable normal tissue.
†Paired *t* testing with Bonferroni adjustment for multiple comparisons ($n = 7$) and capped at 1.00.
‡$n = 19$ on ^{64}Cu-DOTATATE PET at 3 h after injection (one additional lymph node lesion detected in 1 patient).
Data are mean values followed by 95% confidence interval in brackets.

CONCLUSION

^{64}Cu-DOTATATE PET/CT has excellent performance from 1 to 3 h after injection for imaging patients with NENs, with no significant differences in the number of lesions detected. The maintained lesion detection rate and high contrast from 1 to 3 h, combined with the 24-h shelf life, adds to the convenience and flexibility of using ^{64}Cu-DOTATATE PET for routine imaging of patients with NENs.

DISCLOSURE

This project received funding from the European Union's Horizon 2020 research and innovation program under grants 670261 (ERC Advanced Grant) and 668532 (Click-It) and from the Lundbeck Foundation, the Novo Nordisk Foundation, the Innovation Fund Denmark, the Danish Cancer Society, the Arvid Nilsson Foundation, the Svend Andersen Foundation, the Neye Foundation, the Research Foundation of Rigshospitalet, the Danish National Research Foundation (grant 126), the Research Council of the Capital Region of Denmark, the Danish Health Authority, the John and Birthe Meyer Foundation, and the Research Council for Independent Research. Andreas Kjaer and Ulrich Knigge are inventors on patents or applications covering PET tracers for imaging of neuroendocrine tumors. No other potential conflict of interest relevant to this article was reported.

ACKNOWLEDGMENT

We are grateful to the staff at the Department of Clinical Physiology, Nuclear Medicine, and PET for help with performing the PET/CT studies.

KEY POINTS

QUESTION: Can the imaging time window for ^{64}Cu-DOTATATE PET be expanded from 1 h to 1–3 h after injection in patients with NENs?

PERTINENT FINDINGS: ^{64}Cu-DOTATATE PET/CT has excellent performance, with high TTN and conserved lesion detection ability, from 1 to 3 h after injection in patients with NENs.

IMPLICATIONS FOR PATIENT CARE: The imaging time window can be expanded from 1 h to 1–3 h after injection, thus adding to the convenience and flexibility of using ^{64}Cu-DOTATATE PET for routine imaging in patients with NENs.

REFERENCES

1. Yao JC, Hassan M, Phan A, et al. One hundred years after "carcinoid": epidemiology of and prognostic factors for neuroendocrine tumors in 35,825 cases in the United States. *J Clin Oncol.* 2008;26:3063–3072.
2. Papotti M, Croce S, Macri L, et al. Correlative immunohistochemical and reverse transcriptase polymerase chain reaction analysis of somatostatin receptor type 2 in neuroendocrine tumors of the lung. *Diagn Mol Pathol.* 2000;9:47–57.
3. Oberg KE, Reubi JC, Kwekkeboom DJ, Krenning EP. Role of somatostatins in gastroenteropancreatic neuroendocrine tumor development and therapy. *Gastroenterology.* 2010;139:742–753.
4. Sundin A, Arnold R, Baudin E, et al. ENETS consensus guidelines for the standards of care in neuroendocrine tumors: radiological, nuclear medicine & hybrid imaging. *Neuroendocrinology.* 2017;105:212–244.
5. Strosberg JR, Halfdanarson TR, Bellizzi AM, et al. The North American neuroendocrine tumor society consensus guidelines for surveillance and medical management of midgut neuroendocrine tumors. *Pancreas.* 2017;46:707–714.

6. Janson ET, Sorbye H, Welin S, et al. Nordic guidelines 2014 for diagnosis and treatment of gastroenteropancreatic neuroendocrine neoplasms. *Acta Oncol.* 2014;53:1284–1297.
7. Bozkurt MF, Virgolini I, Balogova S, et al. Guideline for PET/CT imaging of neuroendocrine neoplasms with ^{68}Ga-DOTA-conjugated somatostatin receptor targeting peptides and ^{18}F-DOPA. *Eur J Nucl Med Mol Imaging.* 2017;44:1588–1601.
8. Pfeifer A, Knigge U, Binderup T, et al. ^{64}Cu-DOTATATE PET for neuroendocrine tumors: a prospective head-to-head comparison with ^{111}In-DTPA-octreotide in 112 patients. *J Nucl Med.* 2015;56:847–854.
9. Johnbeck CB, Knigge U, Loft A, et al. Head-to-head comparison of ^{64}Cu-DOTATATE and ^{68}Ga-DOTATOC PET/CT: a prospective study of 59 patients with neuroendocrine tumors. *J Nucl Med.* 2017;58:451–457.
10. Jødal L, Le Loirec C, Champion C. Positron range in PET imaging: non-conventional isotopes. *Phys Med Biol.* 2014;59:7419–7434.
11. Bailey DL, Maisey MN, Townsend DW, Valk PE. *Positron emission tomography.* Vol. 2. London, U.K.: Springer; 2005:22.
12. Pfeifer A, Knigge U, Mortensen J, et al. Clinical PET of neuroendocrine tumors using ^{64}Cu-DOTATATE: first-in-humans study. *J Nucl Med.* 2012;53:1207–1215.
13. Bland JM, Altman DG. Multiple significance tests: the Bonferroni method. *BMJ.* 1995;310:170.
14. Rindi G, Kloppel G, Alhman H, et al. TNM staging of foregut (neuro)endocrine tumors: a consensus proposal including a grading system. *Virchows Arch.* 2006;449:395–401.
15. Putzer D, Gabriel M, Henninger B, et al. Bone metastases in patients with neuroendocrine tumor: ^{68}Ga-DOTA-Tyr3-octreotide PET in comparison to CT and bone scintigraphy. *J Nucl Med.* 2009;50:1214–1221.
16. Albanus DR, Apitzsch J, Erdem Z, et al. Clinical value of ^{68}Ga-DOTATATE-PET/CT compared to stand-alone contrast enhanced CT for the detection of extra-hepatic metastases in patients with neuroendocrine tumours (NET). *Eur J Radiol.* 2015;84:1866–1872.
17. Hicks RJ, Jackson P, Kong G, et al. ^{64}Cu-SARTATE PET imaging of patients with neuroendocrine tumors demonstrates high tumor uptake and retention, potentially allowing prospective dosimetry for peptide receptor radionuclide therapy. *J Nucl Med.* 2019;60:777–785.
18. Kunikowska J, Krolicki L, Pawlak D, Zerizer I, Mikolajczak R. Semiquantitative analysis and characterization of physiological biodistribution of ^{68}Ga-DOTA-TATE PET/CT. *Clin Nucl Med.* 2012;37:1052–1057.
19. Shastry M, Kayani I, Wild D, et al. Distribution pattern of ^{68}Ga-DOTATATE in disease-free patients. *Nucl Med Commun.* 2010;31:1025–1032.
20. ter Voert EE, van Laarhoven HW, Kok PJ, Oyen WJ, Visser EP, de Geus-Oei LF. Comparison of liver SUV using unenhanced CT versus contrast-enhanced CT for attenuation correction in ^{18}F-FDG PET/CT. *Nucl Med Commun.* 2014;35:472–477.
21. Yau Y-Y, Chan W-S, Tam Y-M, et al. Application of intravenous contrast in PET/CT: does it really introduce significant attenuation correction error? *J Nucl Med.* 2005;46:283–291.